Supporting Information for

Characterizing precipitation and improving rainfall estimates over the Southern Ocean using ship-borne disdrometer and dual-polarimetric C-band radar

L. G. B. Aragon[1,2,3], Y. Huang[1,2], P. T. May[4], J. Crosier[3,5], E. Montoya Duque[1,2], P. J. Connolly[3], K. N. Bower[3]

[1] School of Geography, Earth and Atmospheric Sciences, The University of Melbourne, Melbourne, VIC, Australia

[2] Australian Research Council Centre of Excellence for Climate Extremes, Melbourne, VIC, Australia

[3] Centre for Atmospheric Science, Department of Earth and Environmental Sciences, The University of Manchester, Manchester, UK

[4] School of Earth, Atmosphere and Environment, Monash University, Clayton, VIC, Australia

[5] National Centre for Atmospheric Science (NCAS), The University of Manchester, Manchester, UK

Contents of this file

Figure S1. Joint frequency distributions of differential reflectivity (ZDR) and cross-correlation coefficient ρHV from OceanPOL precipitation pixels for the seven synoptic types. The -0.4 dB offset factor was already applied in the figure. Most precipitation pixels in M4 and C1 clusters were within the reliable ranges of ZDR values of -4 to 4 dB and ρHV > 0.85, while other synoptic types had higher fractions of precipitation pixels with ρHV < 0.85 that were removed after the quality control procedure (Section 2.2).

Figure S2. Same as Figure S1, but for the joint frequency distributions of ZDR and signal-to-noise ratio (SNR). Most precipitation pixels with SNR < 10 dB were associated with high ZDR spread, and these pixels were also removed after the quality control procedure.

Figure S3. Same as Figure S1, but for the joint frequency distributions of ZDR and horizontal reflectivity (ZH). Higher ZDR spread was found at ZH < 10 dBz, highlighting the difficulty of OceanPOL to differentiate weak meteorological signals from noise.

Figure S4. Mean profiles of temperature (red line), dew-point temperature (blue line), and vector winds plotted in skew-T log-P diagram for the seven synoptic types using hourly ERA5 data that corresponded with available OceanRAIN and OceanPOL data. The shaded regions denote the one standard deviation from the

mean temperatures. The thin red and blue lines denote the temperature values from the k-means centroids of the seven synoptic types from Truong et al. (2020).

Figure S5. Same as Figure 3, but for the Contour frequency by Altitude Diagrams (CFAD) of ZH (second column) and ZDR (third column).

Figure S6. Same as Figure 3 and Figure S5, but for the CFAD and CFTD of ZH and ZDR values from precipitation pixels below 1 km.

Figure S7. Same as Figure 11a, but for the ZH frequency distributions of OceanRAIN and OceanPOL for the different synoptic types.

Table S1. Voyages of the RV Investigator that had measurements of OceanRAIN and OceanPOL south of 43° S.

Additional Supporting Information (Files uploaded separately)

Captions for Animation S1. (a) Synoptic conditions during passage of an extratropical cyclone near the RV Investigator on 18 January 2018. Shown in the figure are the Himawari-8 Channel 13 Brightness temperature (BT); cyclone center and associated fronts; mean sea level pressure contours (solid black lines), surface temperature contours (dashed blue lines), and freezing level height at the ship location (z0 °C at the panel title) from ERA5 data. The green-bordered circle denotes the 150 km radius of OceanPOL. We used each dataset's nearest time offset to the timestamps of available OceanPOL data considering their different temporal resolutions. (b) Surface conditions sampled by OceanRAIN. The evolution of synoptic types at the ship location was shown at the top of the panel. The red vertical dashed line denotes the 11:50 UTC timestamp highlighted in Figure 2. PPI scans of (c) ZH and (d) ZDR at 0.8° elevation. The black dashed circles denote the 1 km refractivity-corrected altitudes. The frame transitions in the animation denote the timestamps of available OceanPOL data.
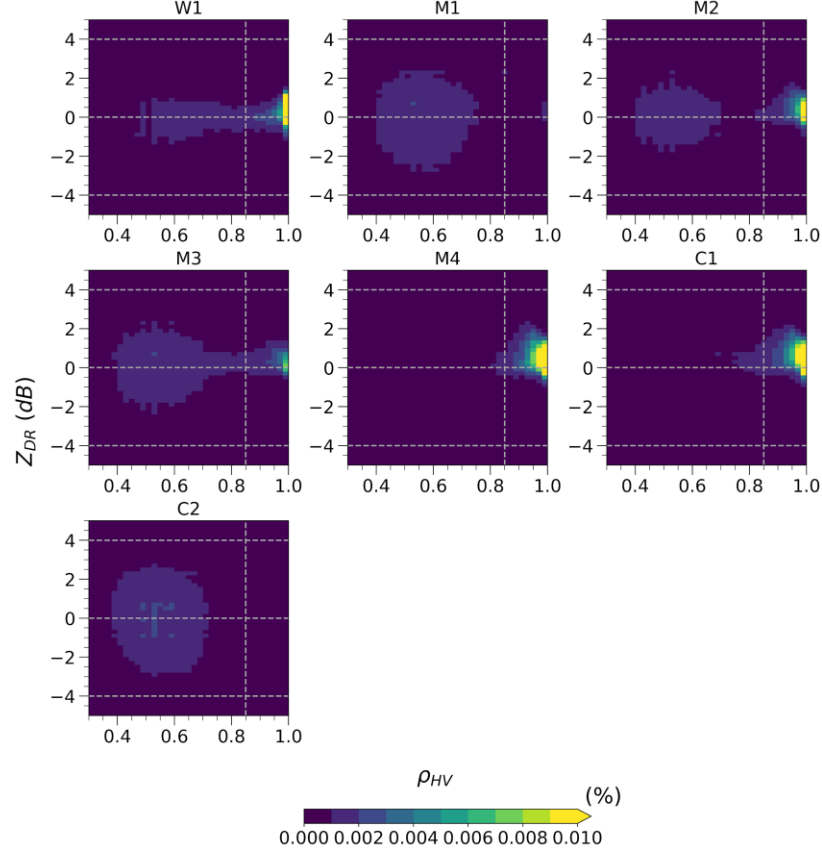
Figure S1. Joint frequency distributions of differential reflectivity (Z_{DR}) and cross-correlation coefficient ρ_{HV} from OceanPOL precipitation pixels for the seven synoptic types. The -0.4 dB offset factor was already applied in the figure. Most precipitation pixels in M4 and C1 clusters were within the reliable ranges of Z_{DR} values of -4 to 4 dB and $\rho_{HV} > 0.85$, while other synoptic types had higher fractions of precipitation pixels with $\rho_{HV} < 0.85$ that were removed after the quality control procedure (Section 2.2).
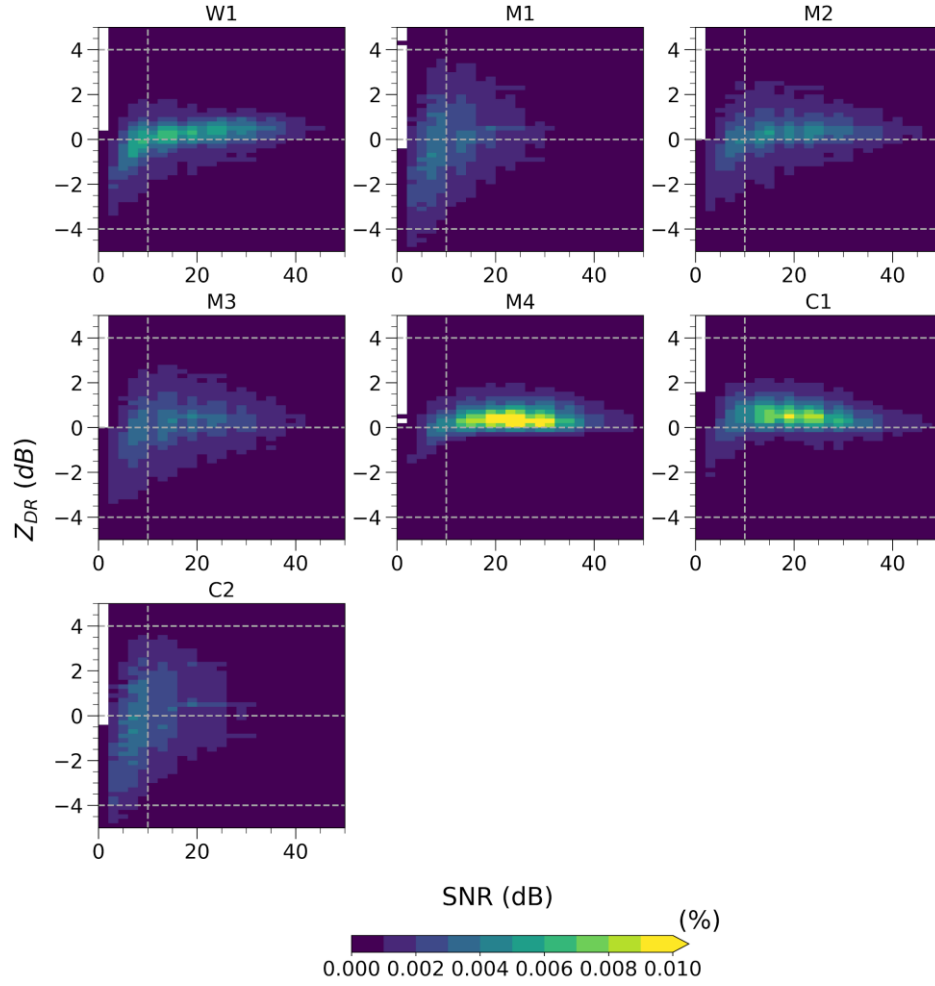
Figure S2. Same as Figure S1, but for the joint frequency distributions of Z_{DR} and signal-to-noise ratio (SNR). Most precipitation pixels with SNR < 10 dB were associated with high Z_{DR} spread, and these pixels were also removed after the quality control procedure.
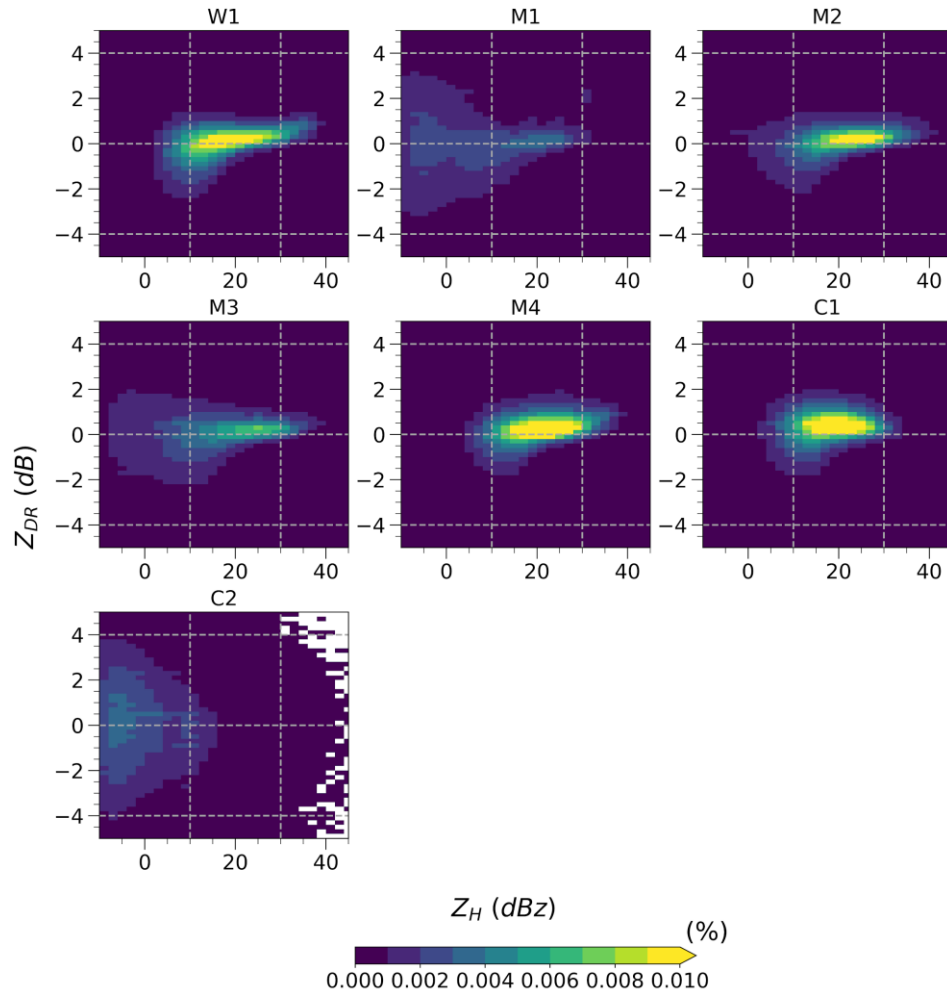
Figure S3. Same as Figure S1, but for the joint frequency distributions of Z_{DR} and horizontal reflectivity (Z_H). Higher Z_{DR} spread was found at $Z_H < 10$ dBz, highlighting the difficulty of OceanPOL to differentiate weak meteorological signals from noise.
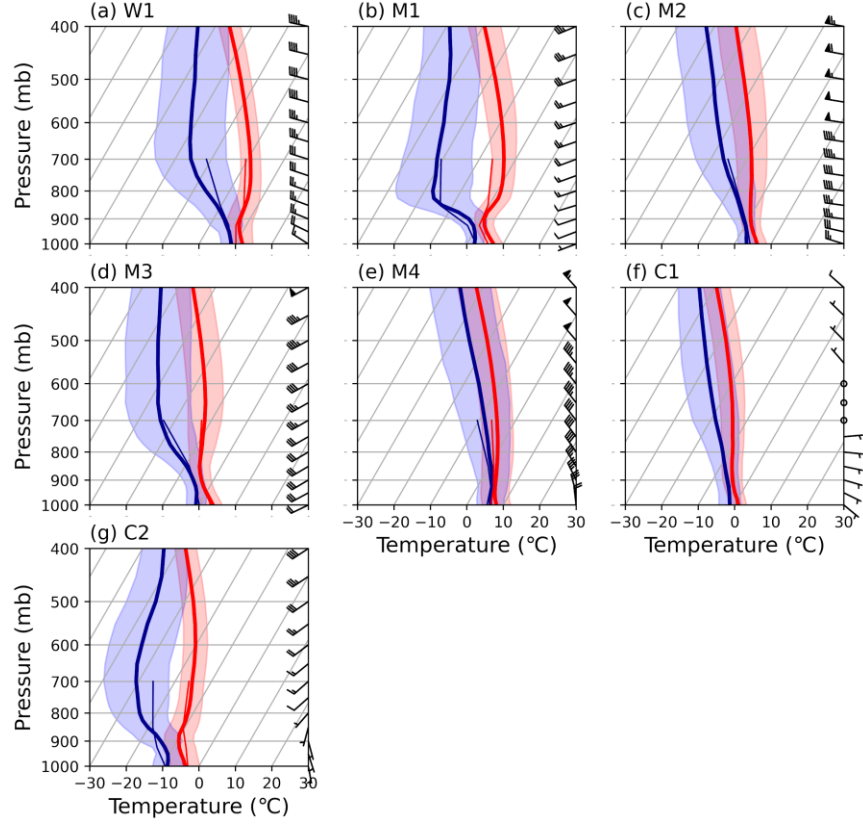
Figure S4. Mean profiles of temperature (red line), dew-point temperature (blue line), and vector winds plotted in skew-T log-P diagram for the seven synoptic types using hourly ERA5 data that corresponded with available OceanRAIN and OceanPOL data. The shaded regions denote the one standard deviation from the mean temperatures. The thin red and blue lines denote the temperature values from the k-means centroids of the seven synoptic types from Truong et al. (2020).
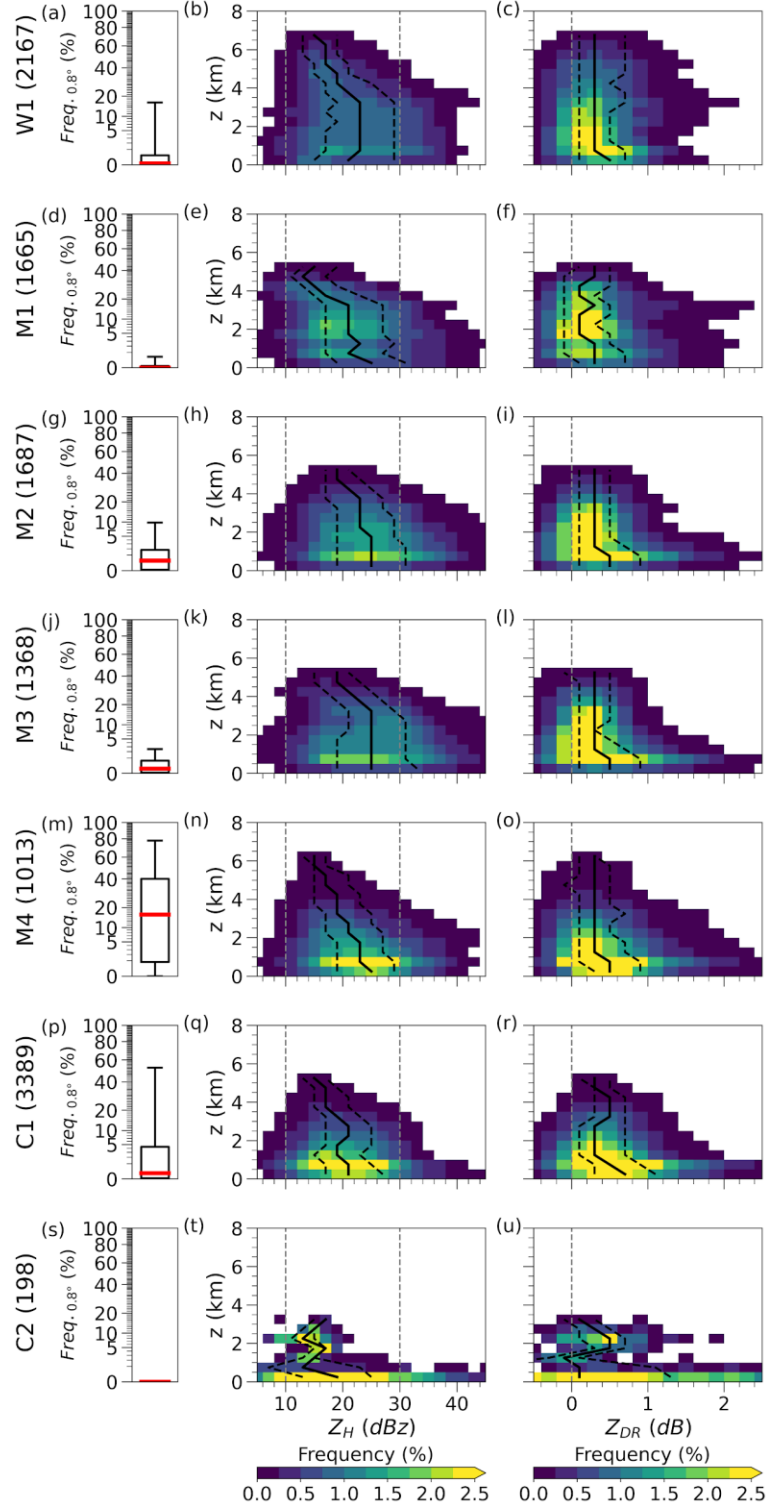
Figure S5. Same as Figure 3, but for the Contour frequency by Altitude Diagrams (CFAD) of Z_H (second column) and Z_{DR} (third column).
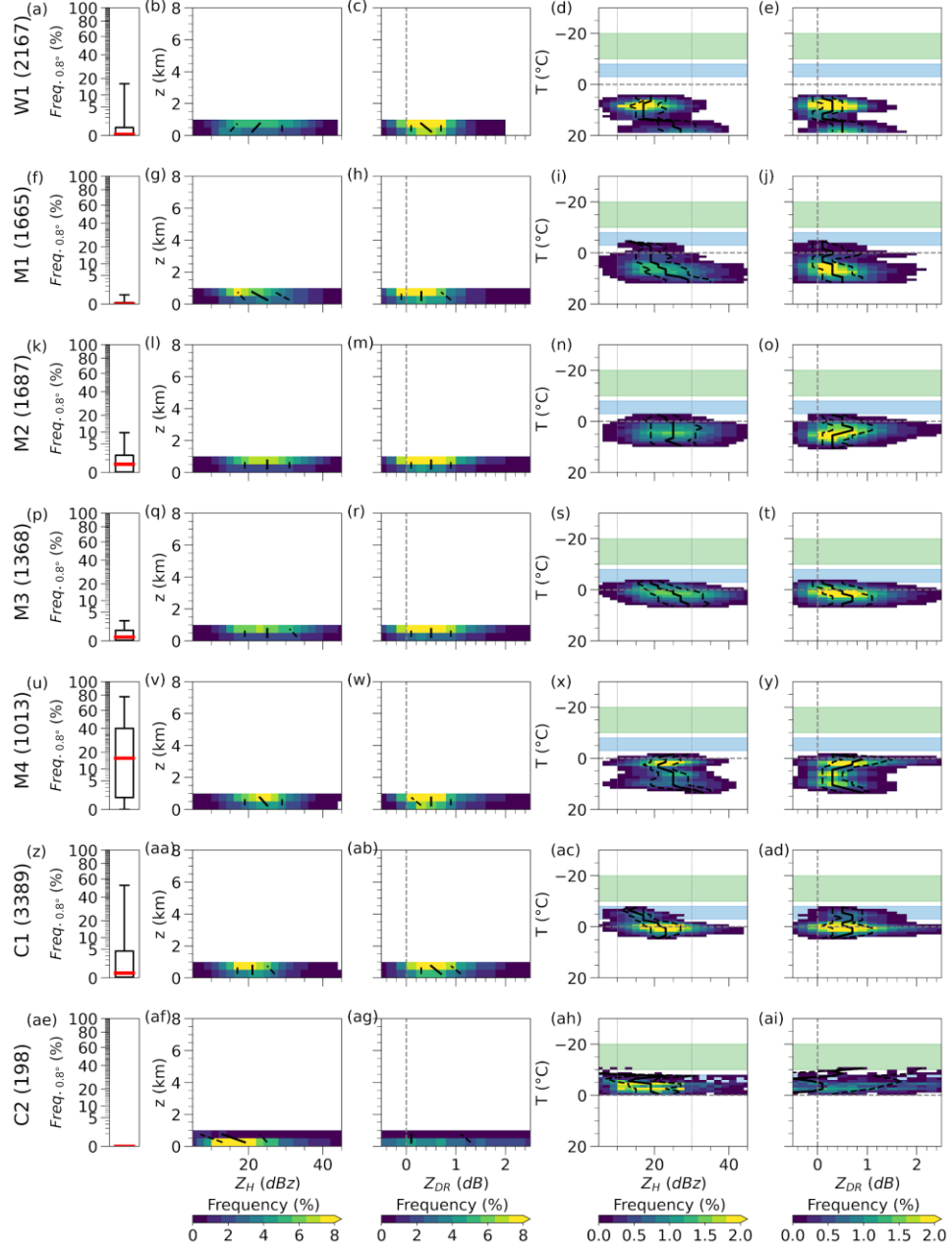
Figure S6. Same as Figure 3 and Figure S5, but for the CFAD and CFTD of Z_H and Z_{DR} values from precipitation pixels below 1 km.
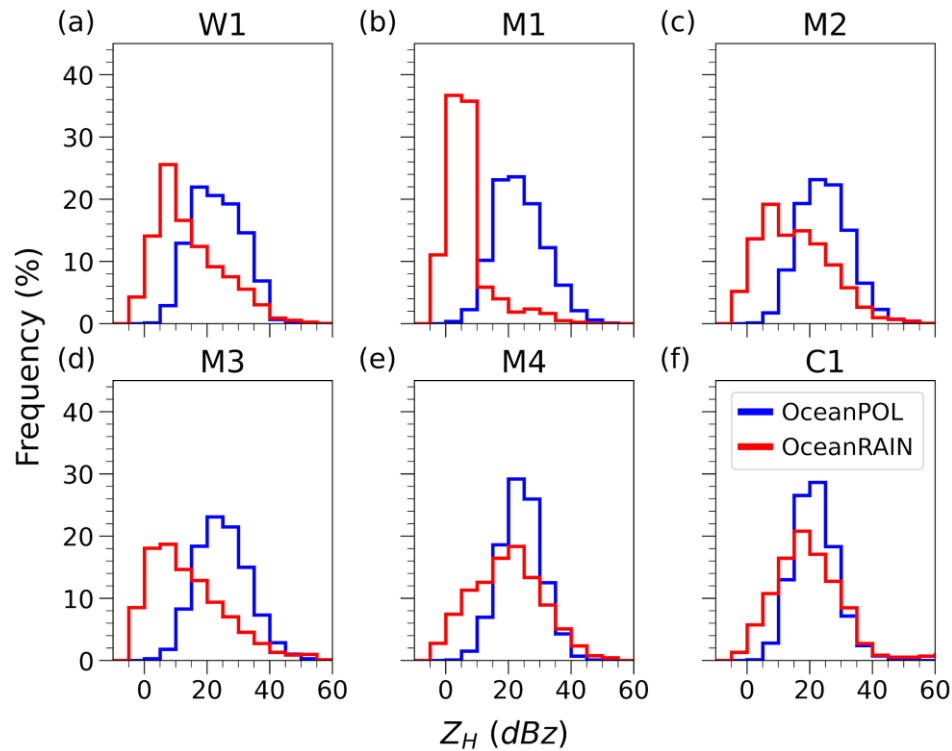
Figure S7. Same as Figure 11a, but for the Z_H frequency distributions of OceanRAIN and OceanPOL for the different synoptic types.

Table S1. Voyages of the RV Investigator that had measurements of OceanRAIN and OceanPOL south of 43° S.

Voyages	Period	OceanRAIN	OceanPOL
IN2016_V01	7 January – 27 Feburary 2016	✓	
IN2016_V02	14 March – 16 April 2016	✓	
IN2016_V03	25 April – 30 June 2016	✓	
IN2017_V01	14 January – 5 March 2017	✓	
IN2017_V02	17–30 March 2017	✓	✓
IN2018_V01	11 January – 22 February 2018	✓	✓
IN2018_V02	3–21 March 2018	✓	✓

Note: The voyage identifiers followed the CSIRO nomenclature, with details available at http://www.marine.csiro.au/data/trawler/survey_list.cfm?source_id=309.

Animation S1. (a) Synoptic conditions during passage of an extratropical cyclone near the RV Investigator on 18 January 2018. Shown in the figure are the Himawari-8 Channel 13 Brightness temperature (BT); cyclone center and associated fronts; mean sea level pressure contours (solid black lines), surface temperature contours (dashed blue lines), and freezing level height at the ship location (z0 °C at the panel title) from ERA5 data. The green-bordered circle denotes the 150 km radius of OceanPOL. We used each dataset's nearest time offset to the timestamps of available OceanPOL data considering their different temporal resolutions. (b) Surface conditions sampled by OceanRAIN. The evolution of synoptic types at the ship location was shown at the top of the panel. The red vertical dashed line denotes the 11:50 UTC timestamp highlighted in Figure 2. PPI scans of (c) ZH and (d) ZDR at 0.8° elevation. The black dashed circles denote the 1 km refractivity-corrected altitudes. The frame transitions in the animation denote the timestamps of available OceanPOL data.